PERGAMON International Journal of Engineering Science 37 (1999) 1351–1367

International Journal of Engineering Science

Two-phase free convection flow over an infinite permeable inclined plate with non-uniform particle-phase density

Hasan M. Ramadan [a], Ali J. Chamkha [b,*]

[a] *Kuwait Airways Corporation, Operations Department, P.O. Box 5447, Salmeya 22065, Kuwait*

[b] *Department of Mechanical and Industrial Engineering, Kuwait University, P.O. Box 5969, Safat 13060, Kuwait*

Received 28 August 1997; accepted 31 August 1998

Abstract

Continuum equations governing steady, laminar, free convection flow of a particulate suspension over an infinite, permeable, inclined and isothermal flat plate are studied. The equations account for particulate viscous and diffusive effects which are absent from most two-phase fluid-particle models. An analytical solution is developed for the particle-phase density distribution. However, the velocity and temperature distributions of both the fluid and particle phases are solved numerically by an implicit finite-difference method. These distributions along with the skin-friction coefficients of both phases and the Nusselt number are illustrated graphically for various parametric conditions. © 1999 Elsevier Science Ltd. All rights reserved.

Keywords: Free convection; Two-phase flow; Suction; Inclined plate; Variable particle-phase density

Nomenclature

c	fluid-phase specific heat
C_f	fluid-phase skin coefficient of friction
D	diffusion coefficient
f	any dependent variable
g	gravitational acceleration
Gr	Grashof number
h	convective heat transfer coefficient
H	dimensionless gravitational acceleration
k	thermal conductivity

* Corresponding author. Tel.: +965 4811 188/5808; fax: +965 4847 131; e-mail: chamkha@kuc01.kuniv.edu.kw.

PII: S0020-7225(98)00117-7

L	characteristic length
N	interphase momentum transfer coefficient
N_T	interphase heat transfer coefficient
Nu	Nusselt number
P	fluid-phase pressure
Pr	fluid-phase Prandtl number
Q_p	dimensionless particle-phase density
Rv	wall suction velocity
Sc	inverse Schmidt number
T	fluid-phase temperature
u	fluid-phase x-component of velocity
U	fluid-phase dimensionless tangential velocity
v	fluid-phase y-component of velocity
V	fluid-phase dimensionless normal velocity
x,y	cartesian coordinates
Y	dimensionless normal distance

Greek symbols

α	velocity inverse Stokes number
β	particle-phase to fluid viscosity ratio
$\bar{\beta}$	volume expansion coefficient
γ	specific heats ratio
ε	temperature inverse Stokes number
θ	fluid-phase dimensionless temperature
κ	particle loading
μ	fluid-phase dynamic viscosity
ν	fluid-phase kinematic viscosity
ρ	fluid-phase density
ϕ	tilt angle
ω	particle-phase wall slip coefficient

Subscripts

$(\ )_n$	numerical scheme grid position index
$(\ )_p$	particle-phase
$(\ )_w$	plate wall
$(\ )_\infty$	very large distance away from the plate surface (ambient condition)

1. Introduction

Convection heat transfer and its related topics are heavily studied fields. These studies range from oversimplified problems to highly complex types of interactions and configurations which require sophisticated numerical schemes and high speed computers to obtain reasonably accurate results. However, the common ground for most of these studies is that they are solved and analyzed by assuming a pure fluid with no contaminants. While this assumption approximates the

reality in some cases quite well, especially for low particle contamination levels, it is not, however, valid in a lot of other cases in which the contaminants in the fluid play a major role in altering the resultant flow and heat transfer characteristics. In many world environments, such as in Kuwait, for example, dust storms or fine dust suspension in the air are encountered for many months during the year. These fine particles of dust penetrate the enclosures and the various devices, and have a serious impact on the performance of many equipments. This example represents a situation of particulate suspension where a pure fluid assumption does not accurately represent the reality. Many other similar situations are faced in such industries as food processing, various grinding operations, settling of various liquid contaminants in large storage tanks, waste processing and recycling, and many others.

There has been considerable work done on various aspects of free-convection flow of a clean fluid over vertical and inclined surfaces. The book by Gebhart et al. [1] summarizes a huge amount of the work done on natural convection in many geometries and for various hydrodynamic and thermal conditions. Other references dealing with free convection from a heated plate for a single-phase flow have been studied by many investigators (see, Refs. [2–6]).

A survey of the technical literature concluded that no work has been done on the problem of free or natural convection heat transfer from surfaces for a particulate (fluid-particle) suspension. However, some work has been found regarding natural convection for liquid–gas mixtures [7]. In addition, there has been considerable work concerning forced convection heat transfer problems for a two-phase particulate suspension (see, for example, Refs. [8–10]).

Recently, the present authors [11] have reported analytical solutions for free convection flow of a particulate suspension past an infinite permeable vertical plate. In those solutions the particle-phase density distribution was assumed to be uniform in the whole domain of interest. This assumption greatly simplified the governing equations which in turn facilitated the development of the analytical solutions. This paper is an extension to the above referenced work. In the present work, the particle-phase density distribution is assumed to be non-uniform. This assumption will result in a set of nonlinear ordinary differential equations from which only the particle-phase density distribution possess an analytical solution whereas the remaining equations must be solved numerically.

2. Problem description and governing equations

Consider steady, laminar, free convection flow of a particulate suspension along an isothermal, inclined, and permeable infinite plate. Far from the plate surface, the ambient fluid is stagnant and the particles are being pulled down by gravitational forces. Uniform fluid-phase suction is imposed at the plate surface. The fluid phase is assumed to be Newtonian, viscous and has constant properties except the density in the buoyancy term. The particle-phase is assumed to consist of solid spherical particles having the same size and that its density distribution is non-uniform. In addition, the particle-phase is assumed viscous, diffusive, and has no analog pressure.

The plate is free to tilt around its lower base in the range of $\pm 60^\circ$ from the vertical position. An energy source, within the plate itself, will maintain the plate wall temperature at a constant value, T_w at all times. T_w will be greater than T_∞ at all times. Fig. 1 shows the general configuration of the problem under consideration.

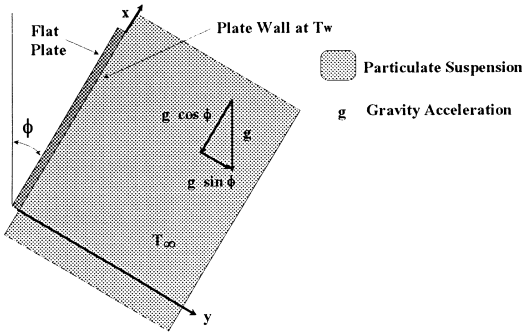

Fig. 1. The general configuration of the problem.

Both the fluid and the particle phases are modeled as interacting continua as discussed by Marble [12]. The mass and thermal diffusivity of the particulate suspension are constant throughout. The volume fraction of the suspended particles relative to that of the fluid will be considered small. The governing equations for the problem under consideration are based on the balance laws of mass, linear momentum, and energy for both the fluid and the particle phases. Since the plate is assumed to be infinite, all dependent variables will be functions of the independent variable y. Taking all the previous assumptions into consideration, the governing equations can be written as

$$\frac{\mathrm{d}v}{\mathrm{d}y} = 0, \tag{1}$$

$$\mu\frac{\mathrm{d}^2u}{\mathrm{d}y^2} - \rho v\frac{\mathrm{d}u}{\mathrm{d}y} - \frac{\mathrm{d}P}{\mathrm{d}x} - \rho_\mathrm{p} N(u-u_\mathrm{p}) - \rho g\ \cos\ \phi = 0, \tag{2}$$

$$k\frac{\mathrm{d}^2T}{\mathrm{d}y^2} - \rho c v\frac{\mathrm{d}T}{\mathrm{d}y} + \rho_\mathrm{p} c_\mathrm{p} N_\mathrm{T}(T_\mathrm{p} - T) = 0, \tag{3}$$

$$D_\mathrm{p}\frac{\mathrm{d}^2\rho_\mathrm{p}}{\mathrm{d}y^2} - \frac{\mathrm{d}(\rho_\mathrm{p} v_\mathrm{p})}{\mathrm{d}y} = 0, \tag{4}$$

$$v_\mathrm{p}\frac{\mathrm{d}}{\mathrm{d}y}\left(\rho_\mathrm{p}\frac{\mathrm{d}u_\mathrm{p}}{\mathrm{d}y}\right) - \rho_\mathrm{p} v_\mathrm{p}\frac{\mathrm{d}u_\mathrm{p}}{\mathrm{d}y} + \rho_\mathrm{p} N(u-u_\mathrm{p}) - \rho_\mathrm{p} g\ \cos\ \phi = 0, \tag{5}$$

$$2v_\mathrm{p}\frac{\mathrm{d}}{\mathrm{d}y}\left(\rho_\mathrm{p}\frac{\mathrm{d}v_\mathrm{p}}{\mathrm{d}y}\right) - \rho_\mathrm{p} v_\mathrm{p}\frac{\mathrm{d}v_\mathrm{p}}{\mathrm{d}y} + \rho_\mathrm{p} N(v-v_\mathrm{p}) - \rho_\mathrm{p} g\ \sin\ \phi = 0, \tag{6}$$

$$\frac{k_\mathrm{p}}{\rho_\mathrm{p}}\frac{\mathrm{d}}{\mathrm{d}y}\left(\rho_\mathrm{p}\frac{\mathrm{d}T_\mathrm{p}}{\mathrm{d}y}\right) - \rho_\mathrm{p} c_\mathrm{p} v_\mathrm{p}\frac{\mathrm{d}T_\mathrm{p}}{\mathrm{d}y} - \rho_\mathrm{p} c_\mathrm{p} N_\mathrm{T}(T_\mathrm{P} - T) = 0. \tag{7}$$

The boundary conditions for this problem are given by

$$
\begin{aligned}
&v(0) = -v_{\mathrm{w}},\\
&u(0) = 0, \quad u(\infty) = 0,\\
&T(0) = T_{\mathrm{w}}, \quad T(\infty) = T_{\infty},\\
&\rho_{\mathrm{p}}(0) = \rho_{\mathrm{pw}}, \quad \rho_{\mathrm{p}}(\infty) = \rho_{\mathrm{p}\infty},\\
&u_{\mathrm{p}}(0) = \omega_{\mathrm{s}} \left.\frac{\mathrm{d}u_{\mathrm{p}}}{\mathrm{d}y}\right|_{y=0}, \quad u_{\mathrm{p}}(\infty) = -\frac{g}{N}\cos\,\phi,\\
&T_{\mathrm{p}}(0) = T_{\mathrm{w}}, \quad T_{\mathrm{p}}(\infty) = T_{\infty},
\end{aligned}
\tag{8}
$$

where ω_{s} and ρ_{pw} are the dimensional particle-phase wall slip and wall density, respectively. It should be noted that the boundary condition for the particle-phase x-component of velocity is familiar from rarefied gas dynamics and has been used by many previous investigators (see, Refs. [10,13]). Also, it is seen from Eqs. (5) and (6) that the particle-phase is endowed with a viscosity. This can be thought of as a natural consequence of the averaging processes involved in representing a discrete system of particles as a continuum (see, for example, Ref. [14,15]). Also, the particle-phase viscous effects can be used to model particle–particle interaction and particle–wall interaction in relatively dense suspensions. These effects have been investigated previously by many authors such as Tsuo and Gidaspow [16] and Gadiraju et al. [17]. The hydrostatic pressure gradient in Eq. (2) is approximated by

$$
\frac{\mathrm{d}P}{\mathrm{d}x} = \rho_{\mathrm{p}_\infty} N u_{\mathrm{p}_\infty} - \rho_\infty g\,\cos\,\phi, \tag{9}
$$

where

$$
u_{\mathrm{p}_\infty} = -\frac{g\,\cos\,\phi}{N}. \tag{10}
$$

This approximation can be easily obtained by evaluating Eqs. (1)–(7) at $y = \infty$. By using Boussinesq approximation [18] to couple the fluid momentum equation with the temperature field and substituting Eqs. (9) and (10), Eq. (2) can be written as

$$
\mu\frac{\mathrm{d}^2u}{\mathrm{d}y^2} - \rho_\infty v\frac{\mathrm{d}u}{\mathrm{d}y} - \rho_{\mathrm{p}} N(u - u_{\mathrm{p}}) + \rho_{\mathrm{p}_\infty} g\,\cos\,\phi + \rho_\infty g\bar{\beta}(T - T_\infty)\cos\,\phi = 0, \tag{11}
$$

where $\bar{\beta}$ is the volume expansion coefficient.

Eqs. (1), (3)–(7) and (11) constitute the governing equations for the problem. These equations represent a generalization of the dusty-gas equations discussed by Marble [12] to include particle-phase viscosity and diffusivity, and buoyancy effects.

To nondimensionalize the above governing equations, the following dimensionless variables are employed.

$$
\begin{aligned}
&Y=\frac{y\mathrm{Gr}^{1/4}}{L}, \quad U=\frac{uL}{\nu\mathrm{Gr}^{1/2}}, \quad V=\frac{vL}{\nu\mathrm{Gr}^{1/4}},\\
&U_{\mathrm{p}}=\frac{u_{\mathrm{p}}L}{\nu\mathrm{Gr}^{1/2}}, \quad V_{\mathrm{p}}=\frac{v_{\mathrm{p}}L}{\nu\mathrm{Gr}^{1/4}}, \quad \theta=\frac{T-T_\infty}{T_{\mathrm{w}}-T_\infty},\\
&\theta_{\mathrm{p}}=\frac{T_{\mathrm{p}}-T_\infty}{T_{\mathrm{w}}-T_\infty}, \quad Q_{\mathrm{p}}=\frac{\rho_{\mathrm{p}}}{\rho_{\mathrm{p}_\infty}}, \quad \kappa=\frac{\rho_{\mathrm{p}_\infty}}{\rho_\infty},\\
&\alpha=\frac{NL^2}{\nu\mathrm{Gr}^{1/2}}, \quad H=\frac{gL^3}{\nu^2\mathrm{Gr}}, \quad \gamma=\frac{c_{\mathrm{p}}}{c},\\
&\varepsilon=\frac{N_{\mathrm{T}}L^2}{\nu\mathrm{Gr}^{1/2}}, \quad \beta=\frac{\nu_{\mathrm{p}}}{\nu}, \quad \mathrm{Pr}=\frac{\mu c}{k},\\
&\mathrm{Pr}_{\mathrm{p}}=\frac{\mu_{\mathrm{p}}c_{\mathrm{p}}}{k_{\mathrm{p}}}, \quad \mathrm{Sc}=\frac{D_{\mathrm{p}}}{\nu}, \quad \mathrm{Gr}=\frac{g\bar{\beta}(T_{\mathrm{w}}-T_\infty)L^3}{\nu^2}.
\end{aligned}
\tag{12}
$$

When the above defined quantities are substituted in Eqs. (1), (3)–(8) and (11) and after simplifying, the following dimensionless equations and boundary conditions result.

$$\frac{\mathrm{d}V}{\mathrm{d}Y}=0, \tag{13}$$

$$\frac{\mathrm{d}^2U}{\mathrm{d}Y^2}-V\frac{\mathrm{d}U}{\mathrm{d}Y}-\alpha\kappa Q_{\mathrm{p}}(U-U_{\mathrm{p}})+(\kappa H+\theta)\cos\phi=0, \tag{14}$$

$$\mathrm{Pr}^{-1}\frac{\mathrm{d}^2\theta}{\mathrm{d}Y^2}-V\frac{\mathrm{d}\theta}{\mathrm{d}Y}+\gamma\varepsilon\kappa Q_{\mathrm{p}}(\theta_{\mathrm{p}}-\theta)=0, \tag{15}$$

$$\mathrm{Sc}\frac{\mathrm{d}^2Q_{\mathrm{p}}}{\mathrm{d}Y^2}-V_{\mathrm{p}}\frac{\mathrm{d}Q_{\mathrm{p}}}{\mathrm{d}Y}=0, \tag{16}$$

$$\beta Q_{\mathrm{p}}\frac{\mathrm{d}^2U_{\mathrm{p}}}{\mathrm{d}Y^2}+\beta\frac{\mathrm{d}Q_{\mathrm{p}}}{\mathrm{d}Y}\frac{\mathrm{d}U_{\mathrm{p}}}{\mathrm{d}Y}-V_{\mathrm{p}}Q_{\mathrm{p}}\frac{\mathrm{d}U_{\mathrm{p}}}{\mathrm{d}Y}+\alpha Q_{\mathrm{p}}(U-U_{\mathrm{p}})-HQ_{\mathrm{p}}\cos\phi=0, \tag{17}$$

$$2\beta\frac{\mathrm{d}}{\mathrm{d}Y}\left(Q_{\mathrm{p}}\frac{\mathrm{d}V_{\mathrm{p}}}{\mathrm{d}Y}\right)-Q_{\mathrm{p}}V_{\mathrm{p}}\frac{\mathrm{d}V_{\mathrm{p}}}{\mathrm{d}Y}+\alpha Q_{\mathrm{p}}(V-V_{\mathrm{p}})+H\mathrm{Gr}^{1/4}Q_{\mathrm{p}}\sin\phi=0, \tag{18}$$

$$\beta\mathrm{Pr}_{\mathrm{p}}^{-1}Q_{\mathrm{p}}\frac{\mathrm{d}^2\theta_{\mathrm{p}}}{\mathrm{d}Y^2}+\beta\mathrm{Pr}_{\mathrm{p}}^{-1}\frac{\mathrm{d}Q_{\mathrm{p}}}{\mathrm{d}Y}\frac{\mathrm{d}\theta_{\mathrm{p}}}{\mathrm{d}Y}-V_{\mathrm{p}}Q_{\mathrm{p}}\frac{\mathrm{d}\theta_{\mathrm{p}}}{\mathrm{d}Y}+\varepsilon Q_{\mathrm{p}}(\theta-\theta_{\mathrm{p}})=0, \tag{19}$$

$$
\begin{aligned}
&V(0)=-\mathrm{Rv},\\
&U(0)=0, && U(\infty)=0,\\
&\theta(0)=1, && \theta(\infty)=0,\\
&Q_{\mathrm{p}}(0)=Q_{\mathrm{p}0}, && Q_{\mathrm{p}}(\infty)=1,\\
&U_{\mathrm{p}}(0)=\omega\left.\frac{\mathrm{d}U_{\mathrm{p}}}{\mathrm{d}Y}\right|_{Y=0}, && U_{\mathrm{p}}(\infty)=-\frac{H}{\alpha}\cos\phi,\\
&\theta_{\mathrm{p}}(0)=1, && \theta_{\mathrm{p}}(\infty)=0,
\end{aligned}
\tag{20}
$$

where $\mathrm{Rv} = v_w L/(\nu \mathrm{Gr}^{1/4})$, $Q_{p0} = \rho_{pw}/\rho_{p\infty}$ and $\omega = \omega_s \mathrm{Gr}^{1/4}/L$ are the dimensionless fluid-phase suction velocity, particle-phase wall density, and the particle-phase wall slip coefficient, respectively.

The fluid-phase skin friction coefficient C_f, the particle-phase skin friction coefficient C_{fp} and the Nusselt number Nu are important physical properties for this flow and heat transfer situation. They can be defined, respectively, as

$$C_f = \frac{\mu(\mathrm{d}u/\mathrm{d}y)|_{y=0}}{(1/2)\rho(v/L)^2\mathrm{Gr}^{3/4}} = 2\frac{\mathrm{d}U}{\mathrm{d}Y}\bigg|_{Y=0}, \tag{21}$$

$$C_{fp} = \frac{\mu_p(\mathrm{d}u_p/\mathrm{d}y)|_{y=0}}{(1/2)\rho(v/L)^2\mathrm{Gr}^{3/4}} = 2\kappa\beta\frac{\mathrm{d}U_p}{\mathrm{d}Y}\bigg|_{Y=0}, \tag{22}$$

$$\mathrm{Nu} = \frac{hL}{k\mathrm{Gr}^{1/4}} = -\frac{\mathrm{d}\theta}{\mathrm{d}Y}\bigg|_{Y=0}. \tag{23}$$

3. Particle-phase density analytical solution

Integrating Eq. (13) and applying the boundary condition for V yields

$$V = -\mathrm{Rv}. \tag{24}$$

Assuming that V_p is constant throughout the domain of interest, and substituting Eq. (24) into Eq. (18) and rearranging yields

$$V_p = \frac{H}{\alpha}\mathrm{Gr}^{1/4}\sin\,\phi - \mathrm{Rv} = \Pi. \tag{25}$$

Note that Eq. (16) with V_p constant is a linear, second-order, ordinary differential equation which is uncoupled from all other variables and therefore can be solved independently from the other system of equations. The solution of Eq. (16) subject to the boundary conditions for Q_p can be shown to be

$$Q_p = 1 + (Q_{p0} - 1)\exp\left(\frac{\Pi}{\mathrm{Sc}}Y\right). \tag{26}$$

An important observation in the above solution needs further elaboration. For a physically acceptable solution, Eq. (26) requires Π to be always negative. If Π is allowed to attain a positive value, the exponential term in Eq. (26) will grow without limit towards infinity, which is, obviously, not a valid solution. This requirement is essential for the physical validity of the result obtained above. Physically, it means that the particle-phase normal velocity must be negative, i.e. towards the plate, to assure a continuous flow of particles to compensate for the lost particles through the suction action and to sustain the requirement of constant particle-phase density at the wall surface. If Π is allowed to be positive, i.e. away from the plate surface, all the particles will be cleaned away from the vicinity of the plate and the wall boundary condition cannot be met.

4. Numerical technique

After substituting the results obtained in the previous section into the governing equations, the following equations result

$$\frac{d^2U}{dY^2} + \mathrm{Rv}\frac{dU}{dY} - \alpha\kappa Q_p(U - U_p) + (\kappa H + \theta)\cos\ \phi = 0, \tag{27}$$

$$\mathrm{Pr}^{-1}\frac{d^2\theta}{dY^2} + \mathrm{Rv}\frac{d\theta}{dY} + \gamma\varepsilon\kappa Q_p(\theta_p - \theta) = 0, \tag{28}$$

$$\beta Q_p\frac{d^2U_p}{dY^2} + \beta\frac{dQ_p}{dY}\frac{dU_p}{dY} - \Pi Q_p\frac{dU_p}{dY} + \alpha Q_p(U - U_p) - HQ_p\cos\phi = 0, \tag{29}$$

$$\beta\mathrm{Pr}_p^{-1}Q_p\frac{d^2\theta_p}{dY^2} + \beta\mathrm{Pr}_p^{-1}\frac{dQ_p}{dY}\frac{d\theta_p}{dY} - \Pi Q_p\frac{d\theta_p}{dY} + \varepsilon Q_p(\theta - \theta_p) = 0, \tag{30}$$

where

$$\frac{dQ_p}{dY} = \frac{\Pi}{\mathrm{Sc}}(Q_{p0} - 1)\exp\left(\frac{\Pi}{\mathrm{Sc}}Y\right) \tag{31}$$

and Q_p is given by Eq. (26) and Π is given by Eq. (25). The above set of equations is obviously coupled and nonlinear and possess no closed-form solution. Therefore, they must be solved numerically for the flow and heat transfer variables.

To solve the above set of ordinary differential equations, a finite difference approximation is adopted. Eqs. (27)–(30) have the general form as

$$\tau_1 f'' + \tau_2 f' + \tau_3 f + \tau_4 = 0 \tag{32}$$

where f is any dependent variable, the prime denotes a differentiation with respect to Y, and the τ_s' are constants and/or functions of the independent variable. To approximate f' and f'', a central difference representation with constant step size throughout the computational domain is employed. This yields

$$f' = \frac{1}{2\Delta Y}(f_{n+1} - f_{n-1}), \tag{33}$$

$$f'' = \frac{1}{(\Delta Y)^2}(f_{n-1} - 2f_n + f_{n+1}), \tag{34}$$

where ΔY is the step size, and the subscript n corresponds to the nth point in the Y direction as shown in Fig. 2.

Substituting Eqs. (33) and (34) into Eq. (32) and rearranging yields

$$Af_{n-1} + Bf_n + Cf_{n+1} = D, \tag{35}$$

where

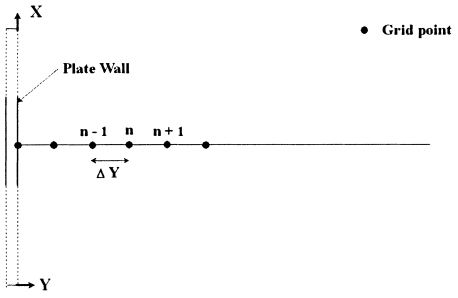

Fig. 2. Finite difference grid representation.

$$A = \frac{1}{\Delta Y}\left(\frac{\tau_1}{\Delta Y} - \frac{\tau_2}{2}\right), \tag{36}$$

$$B = \tau_3 - \frac{2\tau_1}{(\Delta Y)^2}, \tag{37}$$

$$C = \frac{1}{\Delta Y}\left(\frac{\tau_1}{\Delta Y} + \frac{\tau_2}{2}\right), \tag{38}$$

$$D = -\tau_4. \tag{39}$$

When Eq. (35) is repeated for every grid point in the domain, a tridiagonal system of algebraic equations results. The Thomas algorithm is used to solve these algebraic equations (see, Ref. [19]). The solution starts by guessing an initial solution for the variables U, U_p, θ, and θ_p. These values are used to produce a new solution by substituting this initial guess in the respective equations and solving the resulting tridiagonal matrix for each variable in a row. The new solution is then used as an initial guess and the above procedure is repeated for a further modified solution. This procedure is repeated until convergence is achieved. It should be noted that the step size ΔY used in the present work is 0.001. A convergence criterion based on the relative difference between the previous and current iterations was employed. When this difference reached 10^{-7}, the solution was assumed converged and the iteration process was terminated.

5. Results and discussion

Several computer runs were made to study the influence of the various parameters on the case variables. In general, it was noticed that the overall general trends of the solutions were consistent with those which were reported by Chamkha and Ramadan [11] for the same parameters. However, the new parameters introduced in this study showed some effects worth noting. Also, the variations of the particle-phase density modified the effects of parameters already investigated.

The effects of the particle-phase wall density boundary condition, Q_{p0}, are shown in Figs. 3–6. The effect of Q_{p0} on the particle-phase density distribution, which is the result of the analytical solution developed earlier, represented by Eq. (26), is shown in Fig. 3. It is noticed that by increasing the value of Q_{p0}, sharper slopes will result making only a relatively small overall influence

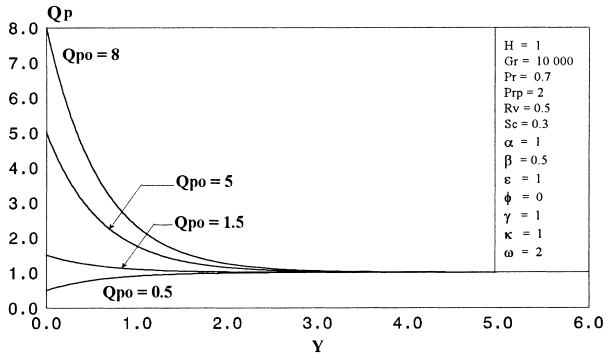

Fig. 3. Effect of Q_{p0} on the particle-phase density profile.

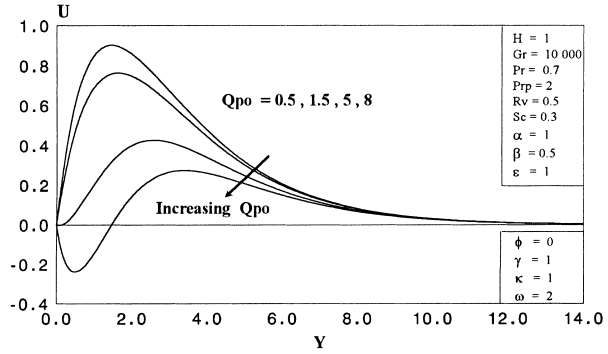

Fig. 4. Effect of Q_{p0} on the fluid velocity profile.

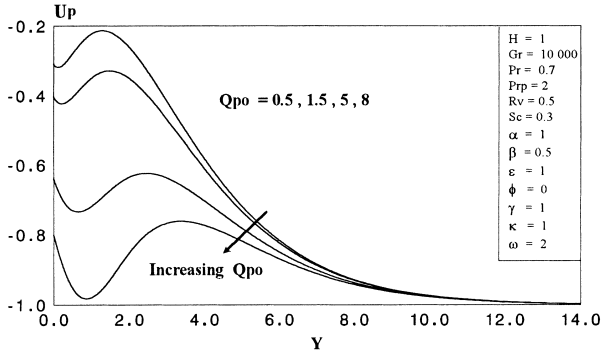

Fig. 5. Effect of Q_{p0} on the particle-phase velocity profile.

on the thickness of the layer where the value of the particle density reaches unity. The same conclusion can be reached by studying Eqs. (26) and (31). The study of Eq. (26) also reveals that the increase in the absolute value of Π, i.e. the increase of the particle-phase normal velocity, will result in a faster decay of the exponential term. The same effect will result with the decrease of the inverse Schmidt number Sc.

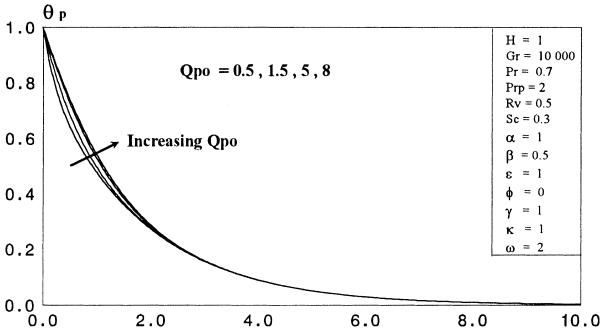

Fig. 6. Effect of Q_{p0} on the particle-phase temperature profile.

Increases in the value of Q_{p0} will produce increases in the amount of drag that the fluid will experience due to the presence of extra mass of the particles and due to the continuous solid–fluid interaction. This drag may be increased by increasing the value of Q_{p0} to a point where the combined effects of the particle drag and inertia will overcome the buoyancy effect and cause the fluid motion to reverse direction. The flow reversal for the fluid phase will continue until such a point where the density of the suspension allows the buoyancy effect to overcome the drag and inertia effects for the particles. This situation is shown clearly in Fig. 4. The effect of Q_{p0} on the particle-phase velocity profile is shown in Fig. 5. As expected, the fluid-phase flow reversal condition discussed earlier for large values of Q_{p0} will cause further retardation of the particle-phase motion as is evident from Fig. 5. The particle-phase temperature profiles are observed to be slightly affected by changes in Q_{p0} as shown in Fig. 6.

The effects of plate tilting are shown in Figs. 7–9. Because the tilt angle influences Π directly, a higher value of the fluid-phase wall suction velocity Rv is used to yield a negative value of Π for the range of all tilt angles considered. Q_{p0} is reduced to show a type of fluid velocity behavior that will be explained below.

Tilt angle influence on the particle-phase density distribution is shown in Fig. 7. The forward tilting of the plate reduces the slope at which the density varies and hence, the density takes a larger distance to attain its ambient boundary condition. It is also noticed that the above effect of the tilting is not linear, i.e. large angles seem to have far greater effect than small to intermediate

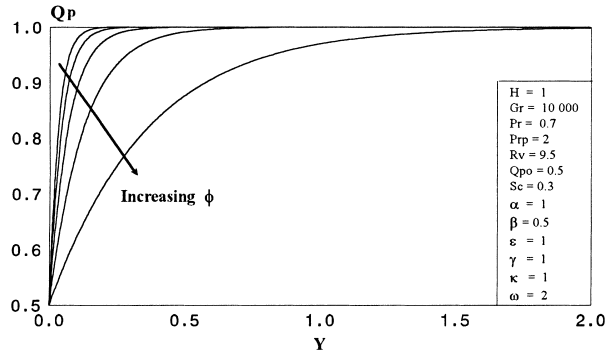

Fig. 7. Effect of the tilt angle on the particle-phase density profile.

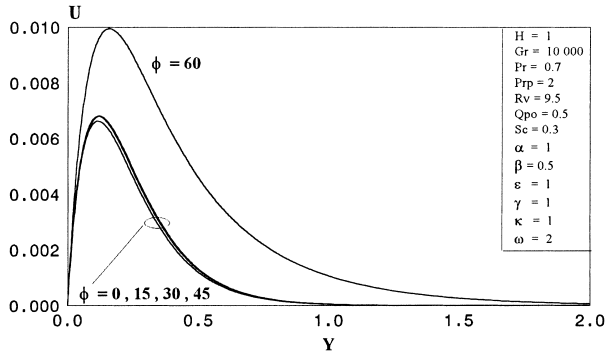

Fig. 8. Effect of the tilt angle on the fluid velocity profile.

angles. This observation is the key to analyze Fig. 8. This figure shows almost unaffected fluid velocity profiles for the range 0°–45° tilt angles. However, the fluid velocity profile is enhanced at the tilt angle of 60°. Owing to the presence of the particles, this observation seems to contradict the results reported by many references (see, Refs. [1,6,20]) for single-phase flow. However, this type of trend could be explained with the aid of Fig. 7. Note that, at any given fixed point relative to the plate (constant Y), as the tilt angle increases, the particle-phase density decreases at this point. Although it is known that tilting of the plate will reduce the buoyancy tangential effect ($\rho g \cos \phi$), this tendency, however, is met with a reduction in the drag from the particles due to the reduced particle-phase density at the same location. These two criteria seem to balance each other to produce almost constant fluid-phase velocity profiles for small to intermediate angles. At large angles ($\phi = 60°$) the particle-phase density profile follows a relatively far smaller slope as explained earlier. As a result, the drag is greatly reduced at the same relative point from the plate. This reduction in drag outweighs the reduction in buoyancy effect and results in what seems to be an enhanced velocity profile at larger angles.

Because of the amount of suction needed to keep Π negative for all values of tilt angles, the velocity profiles are damped and the various layer thicknesses are greatly reduced. Fig. 9 shows that changes in ϕ impact the particle-phase temperature distribution more than the velocity field and that θ_p increases as ϕ increases.

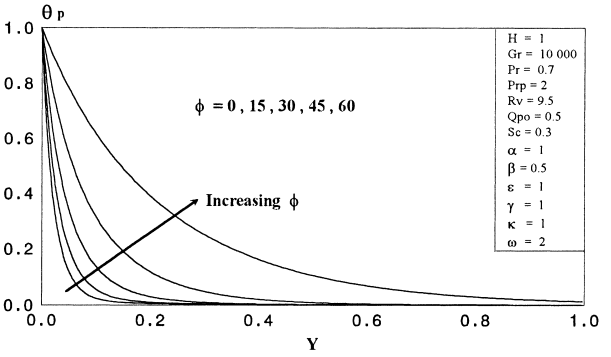

Fig. 9. Effect of the tilt angle on the particle-phase temperature profile.

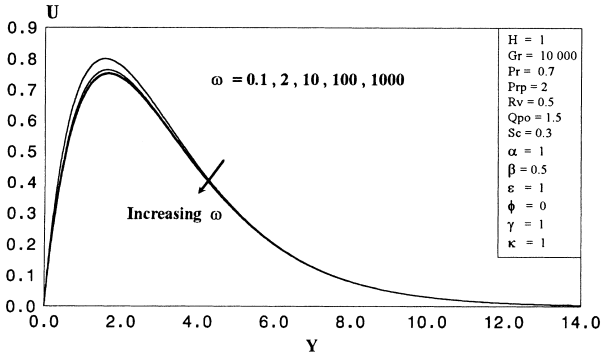

Fig. 10. Effect of ω on the fluid velocity profile.

The effects of the particle-phase wall slip coefficient, ω, are shown in Figs. 10 and 11. In Fig. 10 the influence of ω on the fluid-phase tangential velocity can be seen to be very minor. The effects of ω on the temperature profiles of both phases are also negligible. For this reason, no figures are provided for θ and θ_p. The effect of ω on the particle-phase tangential velocity profiles is shown in Fig. 11. As expected, the wall condition for U_p is highly influenced. However, for values of ω above 100, no changes are noticed in the particle-phase velocity. This means that the perfect slip condition is reached at $\omega = 100$. In addition, ω seems to affect the particle-phase velocity profile only for a short distance from the plate, and its influence disappears further away from the plate.

The Grashof number, Gr, will only influence the value of the boundary condition for V_p and hence Π because the way the governing equations were nondimensionalized the Grashof number is implicitly included in the various parameters. The Grashof number is varied over a given range and the results are given in Figs. 12 and 13. Clearly, the fluid phase will be affected only in a minor manner for the reason given above. For the same reason, the variation of Gr represents only an indirect way to alter the value of Π as Eq. (25) suggests, and in this case, the study of the influence of Gr corresponds to the study of the influence of Π on the case variables. To assume a negative value for Π in the whole range of Gr, the wall fluid-phase suction is increased. The plate is tilted forward to include the effect of Gr in the calculation of Π. The effect of Gr on the particle-phase density distribution is shown in Fig. 12. As Gr is increased, the value of Π decreases (for forward

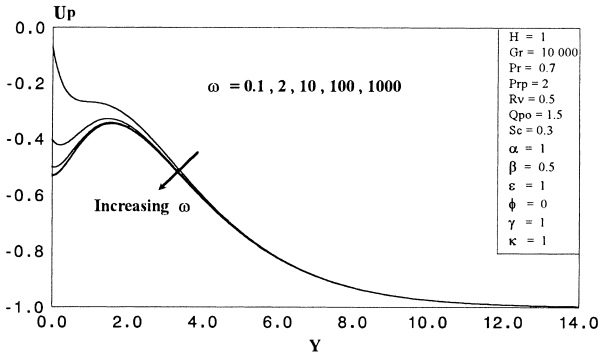

Fig. 11. Effect of ω on the particle-phase velocity profile.

plate tilting), and the exponential term in Eq. (26) will decay more slowly. The effect of increasing Gr is seen to increase the particle-phase temperature as depicted in Fig. 13.

The fluid-phase coefficient of friction decreases with increase in Q_{p0} as shown in Fig. 14. Negative values of C_f occur where the fluid flow reverses direction due to the increased drag and the particle inertia effects. The same trends are observed for the particle-phase coefficient of

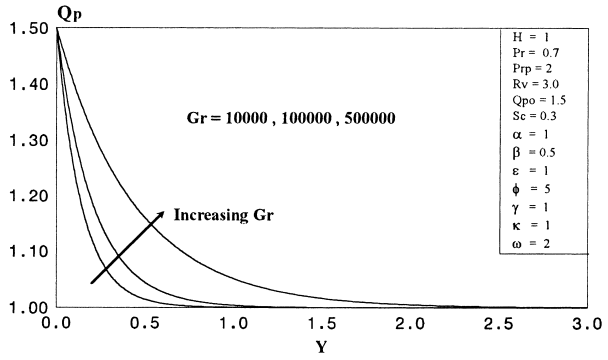

Fig. 12. Effect of Grashof number on the particle-phase density profile.

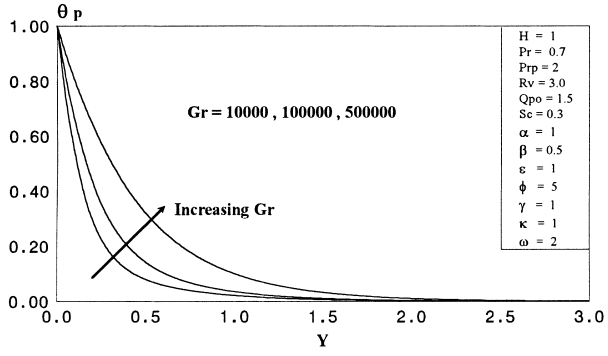

Fig. 13. Effect of Grashof number on the particle-phase temperature profile.

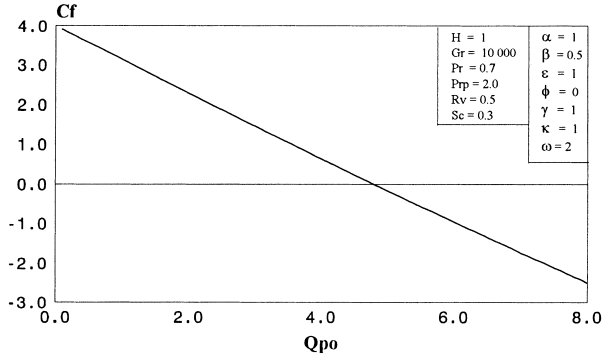

Fig. 14. Effect of Q_{p0} on the fluid-phase coefficient of friction.

friction. The effects of the inverse Schmidt number Sc on the particle-phase coefficient of friction is displayed in Fig. 15. Higher absolute values of C_{fp} are obtained as Sc increases.

Finally, the influences of Sc, Q_{p0}, and ϕ on the Nusselt number Nu are illustrated in Figs. 16–18, respectively. It is observed from these figures that Nu reaches a minimum around Sc = 0.1 and

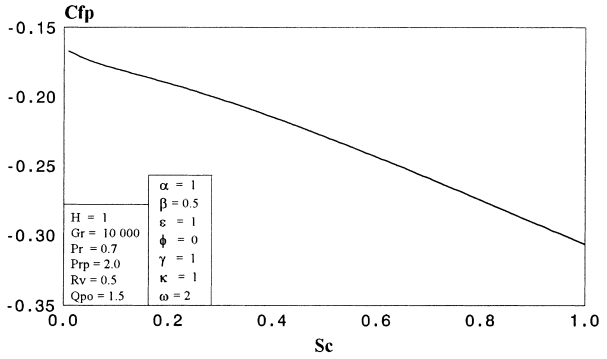

Fig. 15. Effect of Sc on the particle-phase coefficient of friction.

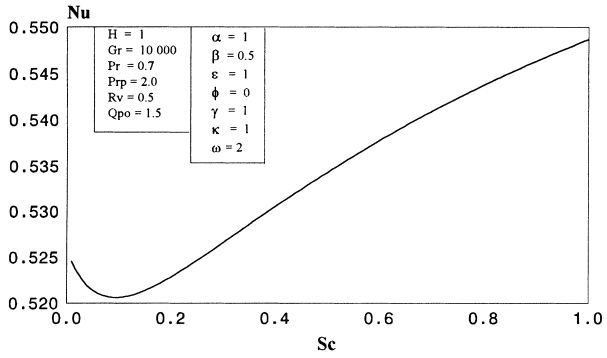

Fig. 16. Effect of Sc on the Nusselt number.

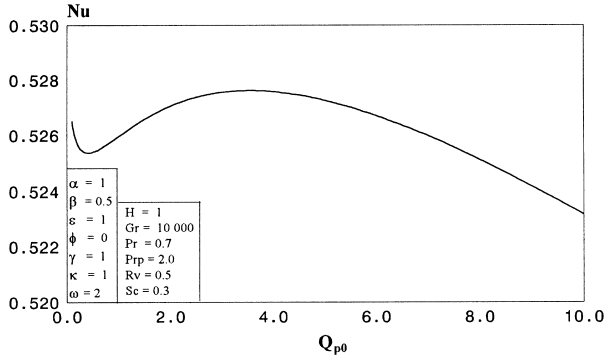

Fig. 17. Effect of Q_{p0} on the Nusselt number.

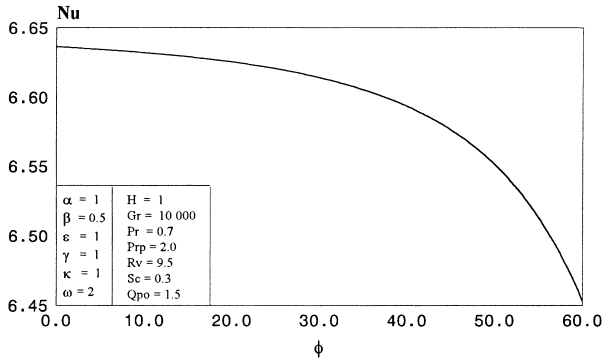

Fig. 18. Effect of ϕ on the Nusselt number.

increases with increasing values of Sc beyond this value. Also, for the parametric values used to obtain Fig. 17, Nu seems to decrease with Q_{p0} except for values of Q_{p0} between 1 and 3.5. In addition, Nu experiences small decreases with increase in the tilt angle ϕ for $0 \leqslant \phi \leqslant 45$. However, for values of $\phi > 45$ sharp decreases in Nu are predicted. This is due to the significant changes in the slopes of the fluid-phase temperature as ϕ is increased beyond $\phi = 45$.

It should be noted that, for a vertical plate ($\phi = 0$) and uniform particle-phase density distribution ($Q_p = 1$), all of the numerical results reported herein are consistent with the analytical solutions reported earlier by Chamkha and Ramadan [11].

6. Conclusion

The mathematical modelling for free convection flow of a particulate suspension over an infinite, inclined, and permeable isothermal plate was studied. The model accounts for particle viscous and diffusive effects. The particle-phase density distribution was assumed to be variable in the whole domain of interest. An analytical solution was developed for the particle-phase density and a numerical solution based on the finite-difference method was obtained for the remaining variables. It was found that the choice of the particle-phase wall density boundary condition greatly influenced the tangential velocity profiles due to the variation of the amount of drag experienced by the fluid phase. It also influenced the Nusselt number. Moreover, it was found that at small values of Q_{p0} the amount of drag balances the reduction in buoyancy effect as the plate is tilted forward at small to intermediate angles. The Nusselt number, however, decreased with forward plate tilting. The slip coefficient and Grashof number effects were also discussed. Representative figures for both phases coefficients of friction showed that the fluid-phase skin-friction coefficient decreased with increasing wall particle-phase density and that the particle-phase coefficient of friction decreased as the inverse Schmidt number was increased. From this and the previous works on this subject, it is concluded that the significant changes in the flow and heat transfer characteristics can result due to the presence of particles. It is hoped that this work and the results reported will stimulate interest in carrying out both theoretical and experimental investigations dealing with natural convection flows of particulate suspensions over and through various geometries.

References

[1] B. Gebhart, Y. Jaluria, R.L. Mahajan, B. Sammakia, Buoyancy-Induced Flows and Transport, Hemisphere, New York, 1988.
[2] E.M. Sparrow, J.L. Gregg, Laminar free convection from a vertical plate with uniform surface heat flux, Trans. ASME 78 (1956) 435.
[3] W.T. Kierkus, An analysis of laminar free convection flow and heat transfer about an inclined isothermal flat plates, Int. J. Heat and Mass Transfer 11 (1968) 241–253.
[4] K. Hassan, S. Mohammed, Natural convection from isothermal flat surfaces, Int. J. Heat and Mass Transfer 13 (1970) 1873–1886.
[5] M.M. Elsayed, K.A. Fathalah, Temperature Distribution in a Direct Solar Heater, 72nd annual meeting of AIChE, Paper No. P-7d, 1979.
[6] T. Fuji, H. Imura, Natural convection heat transfer from a plate with arbitrary inclination, Int. J. Heat and Mass Transfer 15 (1972) 755.
[7] C.Y. Wang, C. Beckermann, C. Fan, Numerical study of boiling and natural convection in capillary porous media using the two-phase mixture model, Int. J. Computation and Methodology 26 (4) (1994) 375–398.
[8] A.J. Chamkha, Convective heat transfer of a particulate suspension, J. Thermophys. and Heat Transfer 6 (1992) 551–553.
[9] A.J. Chamkha, Thermal flat plate boundary-layer solution for a particulate suspension with finite volume fraction, Int. J. Multiphase Flow 19 (3) (1993) 539–540.
[10] S.L. Soo, Particulates And Continuum Multiphase Fluid Dynamics, Hemisphere, Washington, DC, 1989.
[11] A.J. Chamkha, H.M. Ramadan, Analytical solutions for free convection of a particulate suspension past an infinite vertical surface, Int. J. Eng. Science, in press.
[12] F.E. Marble, Dynamics of dusty gases, Annual Rev. Fluid Mech. 2 (1970) 297–446.
[13] A.J. Chamkha, Compressible dusty-gas boundary-Layer flow over a flat surface, ASME J. Fluids Eng. 118 (1996) 179–185.
[14] D.A. Drew, Mathematical modeling of two-phase flow, Annual Rev. Fluid Mech. 15 (1983) 261–291.
[15] D.A. Drew, L.A. Segal, Analysis of fluidized beds and foams using averaged equations, Studies in Appl. Math. 50 (1971) 233–252.
[16] Y.P. Tsuo, D. Gidaspow, Computation of flow patterns in circulating fluidized beds, AIChE J. 36 (1990) 88–896.
[17] M. Gadiraju, J. Peddieson, S. Munukutla, Exact solutions for two-phase vertical pipe flow, Mech. Res. Commun. 19 (1992) 7–13.
[18] A. Bejan, Convection Heat Transfer, 2nd ed., Wiley, New York, 1995.
[19] S.C. Chapra, R.P. Canale, Numerical Methods For Engineers, 2nd ed., McGraw-Hill, New York, 1988.
[20] J.P. Holman, Heat Transfer, McGraw-Hill, New York, 1989.